Supplement of Earth Syst. Dynam., 17, 319–331, 2026
https://doi.org/10.5194/esd-17-319-2026-supplement

Earth System Dynamics
Open Access
EGU

Supplement of

Energetics of monsoons and deserts: role of surface albedo vs water vapor feedback

Chetankumar Jalihal and Uwe Mikolajewicz

Correspondence to: Chetankumar Jalihal (chetankumar.jalihal@mpimet.mpg.de)

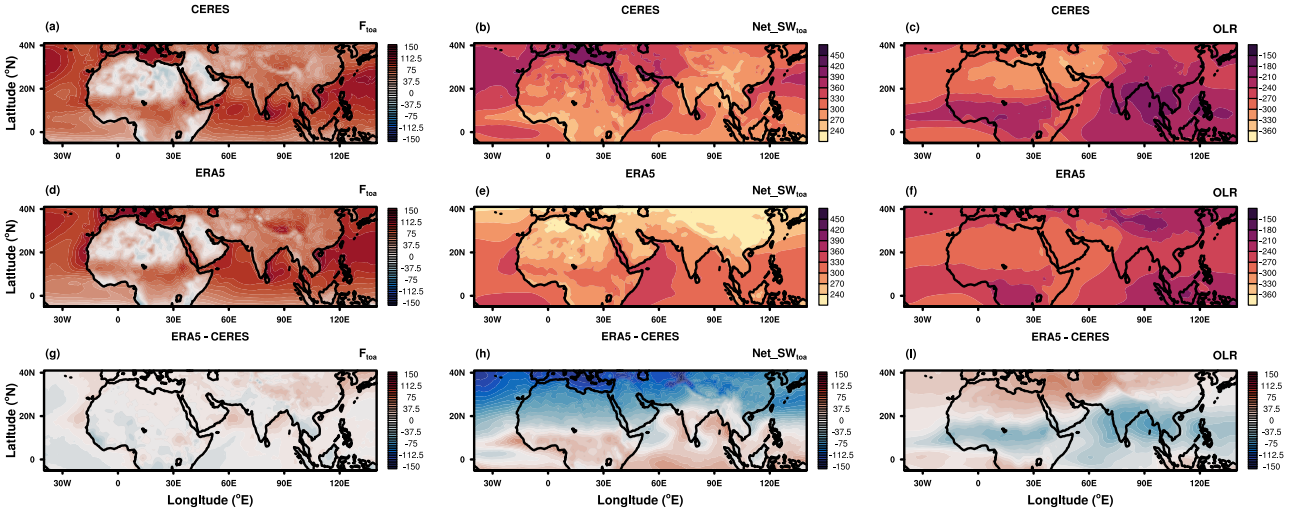

Figure S1. F_{toa} and its components. The spatial distribution of the total energy budget at the top of the atmosphere (F_{toa}) and it's components (in W m^{-2}) is shown by using ERA-5 climatology (1991–2020) and CERES climatology (07/2005–06/2015). The maps represent the Jun-Jul-Aug mean. The top row (**a–c**) displays data from CERES, middle row (**d–f**) depicts the data from ERA-5, and the bottom row (**g-i**) shows the anomaly between ERA-5 and CERES. The left column (**a,d,g**) presents F_{toa}, center column (**b,e,h**) depicts the all-sky net shortwave radiation, and the right column (**c,f,i**) represents the outgoing longwave radiation.

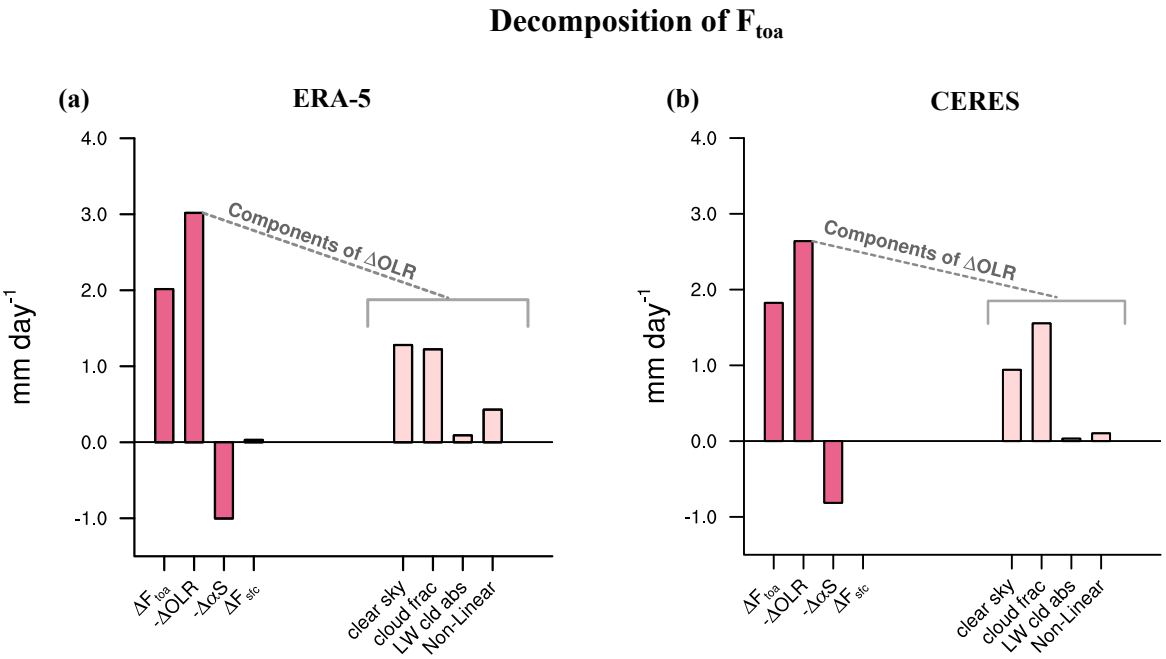

Figure S2. Decomposing F_{toa}. The bar chart illustrates the differences in the TOA fluxes and their components between Sahara and S.Asia. The regions selected for the analysis are shown in the inset map with grey shading in the main Figure 3a: 0°E–30°E and 15°N–30°N; land-only grid points (Sahara) and 70°E–100°E and 15°N–30°N; all grid points (South Asia). (**a**) is taken from ERA-5 climatology (1991–2020) and (**b**) is from CERES. Jun-Jul-Aug means are used for these climatologies.

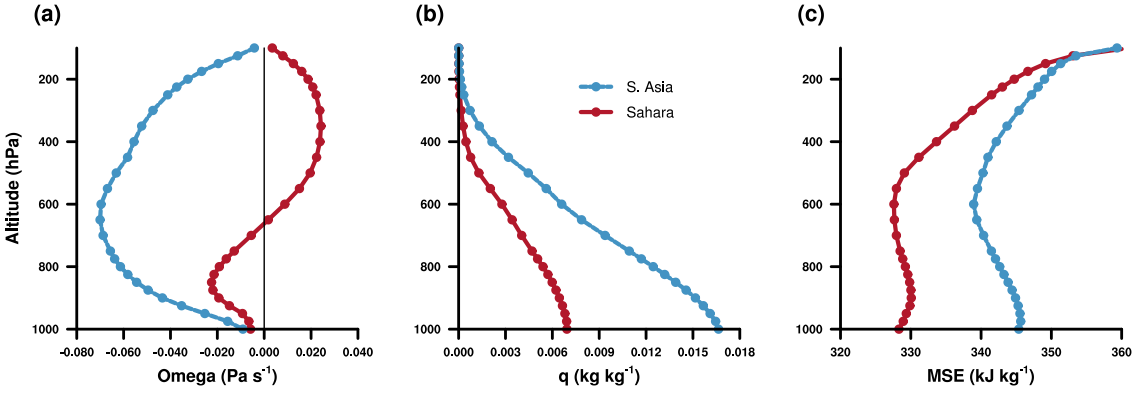

Figure S3. Vertical profiles over monsoons and deserts. Vertical profile of (**a**) vertical pressure velocity, (**b**) specific humidity, and (**c**) moist-static energy. The area-averaged parameters for South Asia (70°E–105°E; 15°N–30°N) and the Sahara (0°E–30°E and 15°N–30°N) are shown in blue and red, respectively. The Jun-Jul-Aug climatology from 1991 to 2020 is obtained from ERA-5.

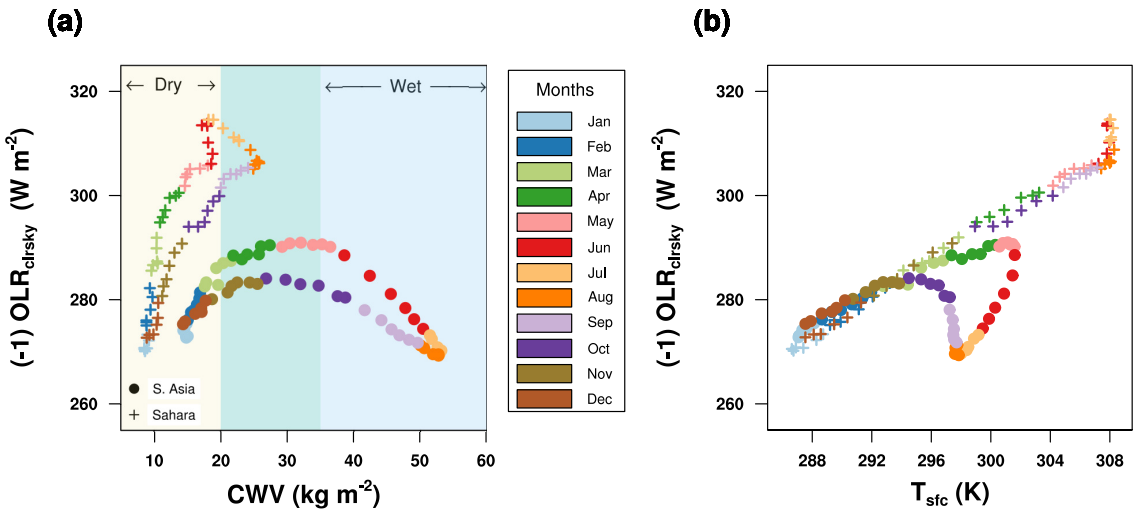

Figure S4. Clear-sky OLR as a function of surface temperature and water vapor in ERA-5. (**a**) & (**b**) illustrate the relation between clear sky OLR, column-integrated water vapor and surface temperature, respectively. Pentad climatology (1991–2020) from ERA-5 are considered. The regions selected for the analysis are shown in the inset map with grey shading in the main Figure 3a: 0°E–30°E and 15°N–30°N; land-only grid points (Sahara) and 70°E–100°E and 15°N–30°N; all grid points (South Asia). The filled circles represent area average parameters over the South Asian domain and the '+' depicts the area average parameters over the Sahara. The colors indicate months of the year. Energy gained by the atmosphere is considered positive; therefore, clear-sky OLR, which represents energy lost to space, is multiplied by -1 to account for this energy loss.

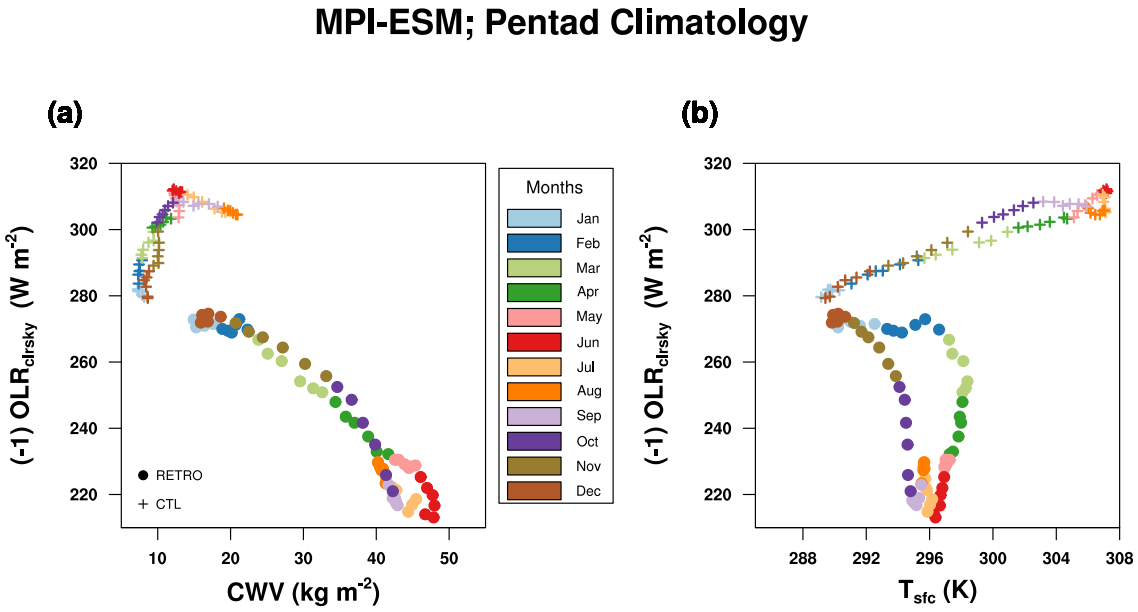

Figure S5. Clear-sky OLR as a function of surface temperature and water vapor over the Sahara in MPI-ESM. (**a**) & (**b**) show a scatter of clear sky OLR with column-integrated water vapor and surface temperature, respectively. Pentad climatology of the last 100 years of the simulation is considered. The region selected for this analysis is shown in the inset map in Figure 6a: 0°E–50°E and 10°N–25°N; land-only grid points. The filled circles represent area average parameters over the Sahara in the RETRO simulation, whereas, the '+' depicts the area average parameters over the Sahara in the CTL simulation. The colors indicate months of the year. Energy gained by the atmosphere is considered positive; therefore, clear-sky OLR, which represents energy lost to space, is multiplied by -1 to account for this energy loss.

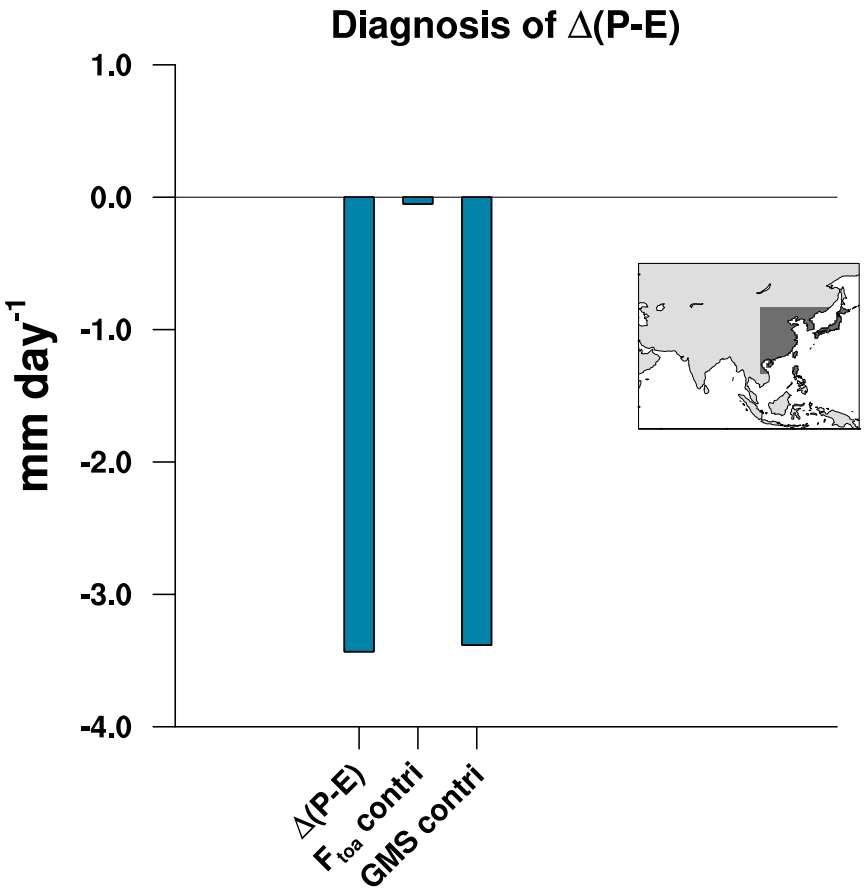

Figure S6. Diagnosis of moisture convergence over South East Asia. Bar graph of change in (Precipitation - Evaporation) P-E, contribution of F_{toa}, and GMS. The changes in Jun-Jul-Aug climatology between RETRO and the CTL over the domain (105°E–150°E and 15°N–45°N; land-only grid points as shown in grey shading in the inset map), is considered for this analysis.

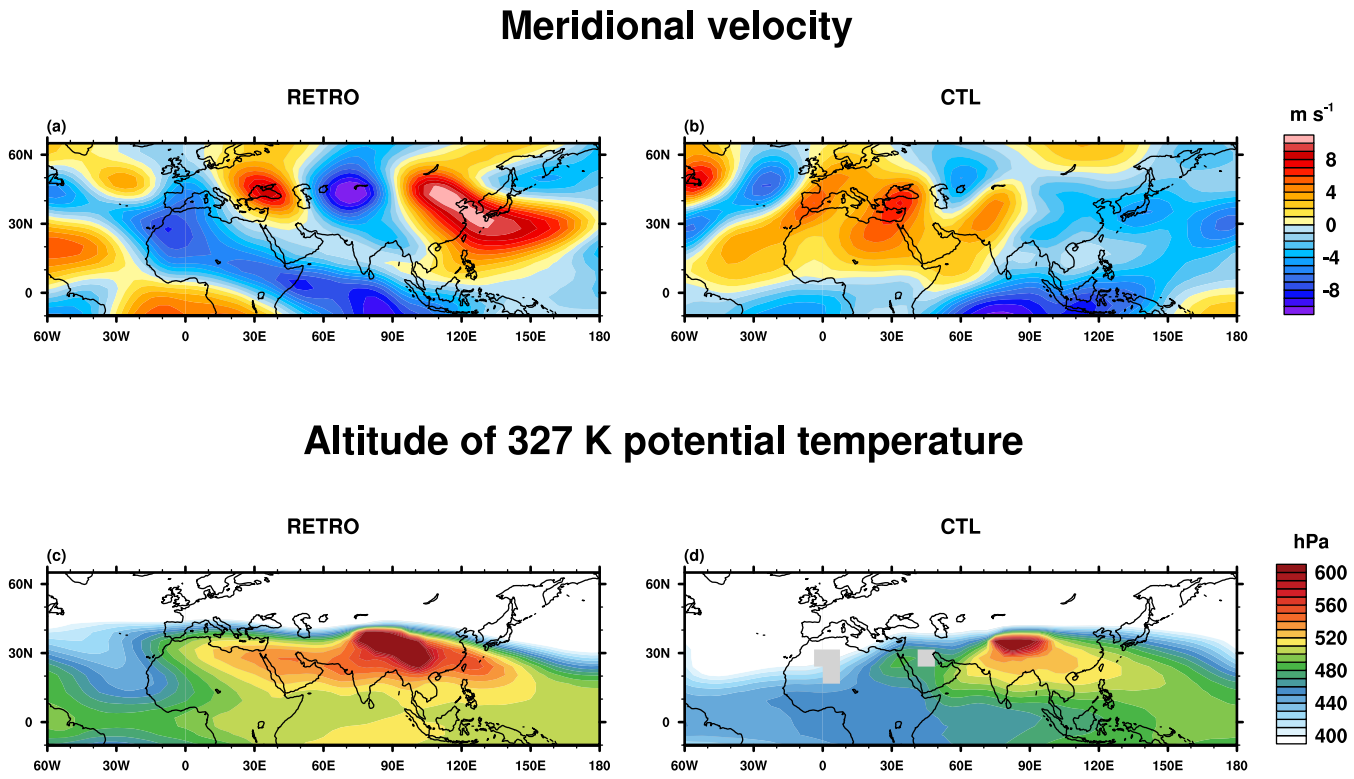

Figure S7. Meridional velocity at 200 hPa and 327 K potential temperature. Spatial maps of (**a**) & (**b**) meridional velocity (200 hPa) and (**c**) & (**d**) the altitude of 327 K potential temperature. (**a**) & (**c**) are from the RETRO simulation, and (**b**) & (**d**) depict the CTL simulation. Jun-Jul-Aug climatology of the last 100-yrs of the simulation are used for these plots.

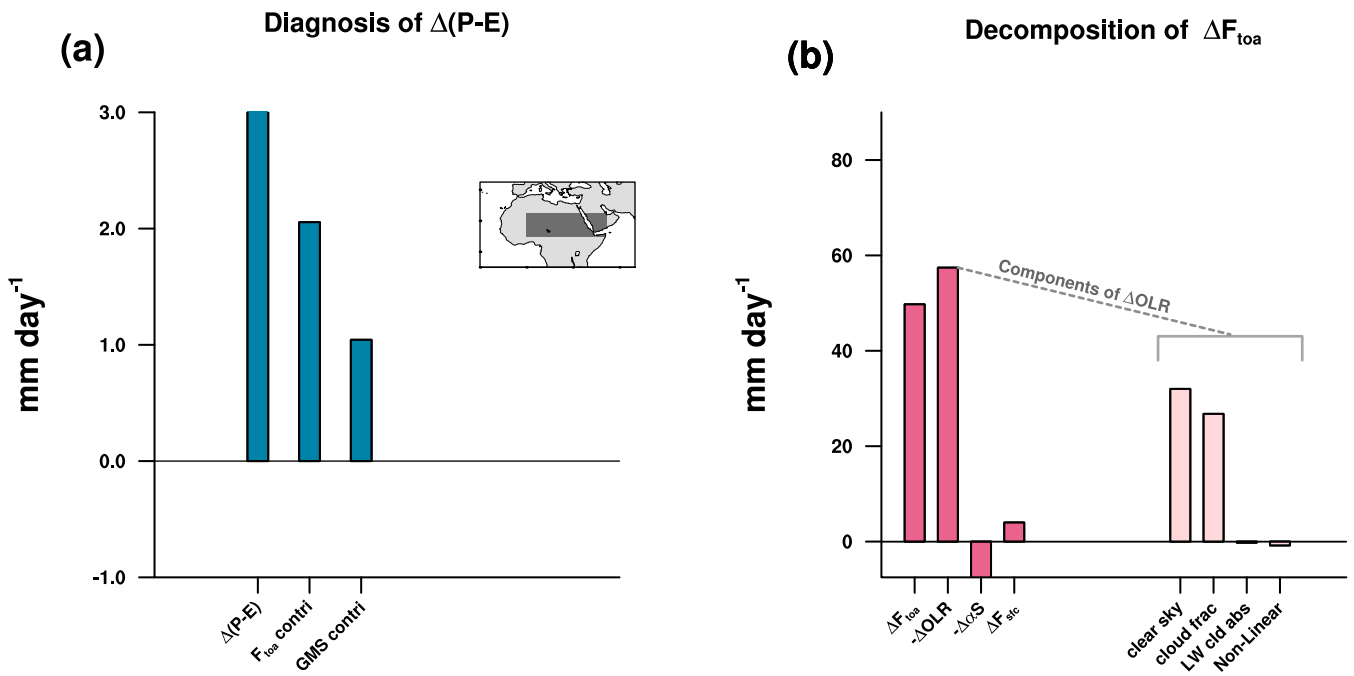

Figure S8. Diagnosis of change in moisture convergence during the first year of RETRO simulation. Bar graph of (**a**) change in (Precipitation - Evaporation; P-E), contribution of F_{toa}, and GMS, & (**b**) the change in F_{toa} and its components (see Data and Methods). The changes between Jun-Jul-Aug average of the first year of simulation from the RETRO and Jun-Jul-Aug climatology from the CTL over the domain (0°E–50°E and 10°N–25°N; land-only grid points as shown in grey shading in the inset map), is considered for this analysis. The change in OLR is further decomposed into changes due to clear sky OLR, changes in cloud area fraction, the longwave cloud absorption, and non-linear term (see Data and Methods).

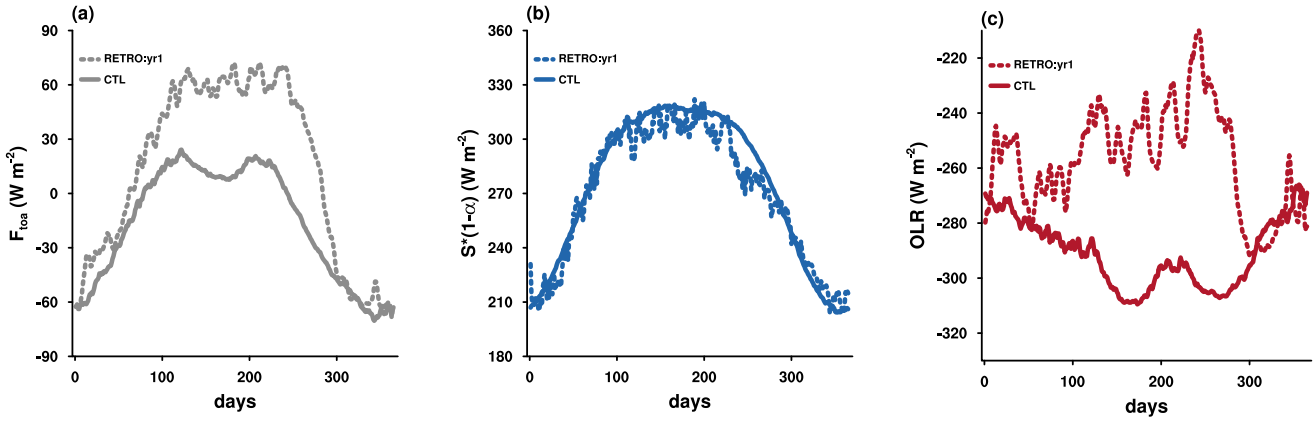

Figure S9. Seasonal cycle of F_{toa} and its components. The time series of (**a**) F_{toa}, (**b**) Net shortwave at the top of atmosphere, and (**c**) outgoing longwave radiation (OLR), area averaged over the domain (0°E–50°E and 10°N–25°N; land-only grid points). The solid line represents the steady-state from CTL, and the dashed line represents the first year of simulation from RETRO. Area average of the daily data is taken. Positive values indicate the energy gained by the atmosphere.

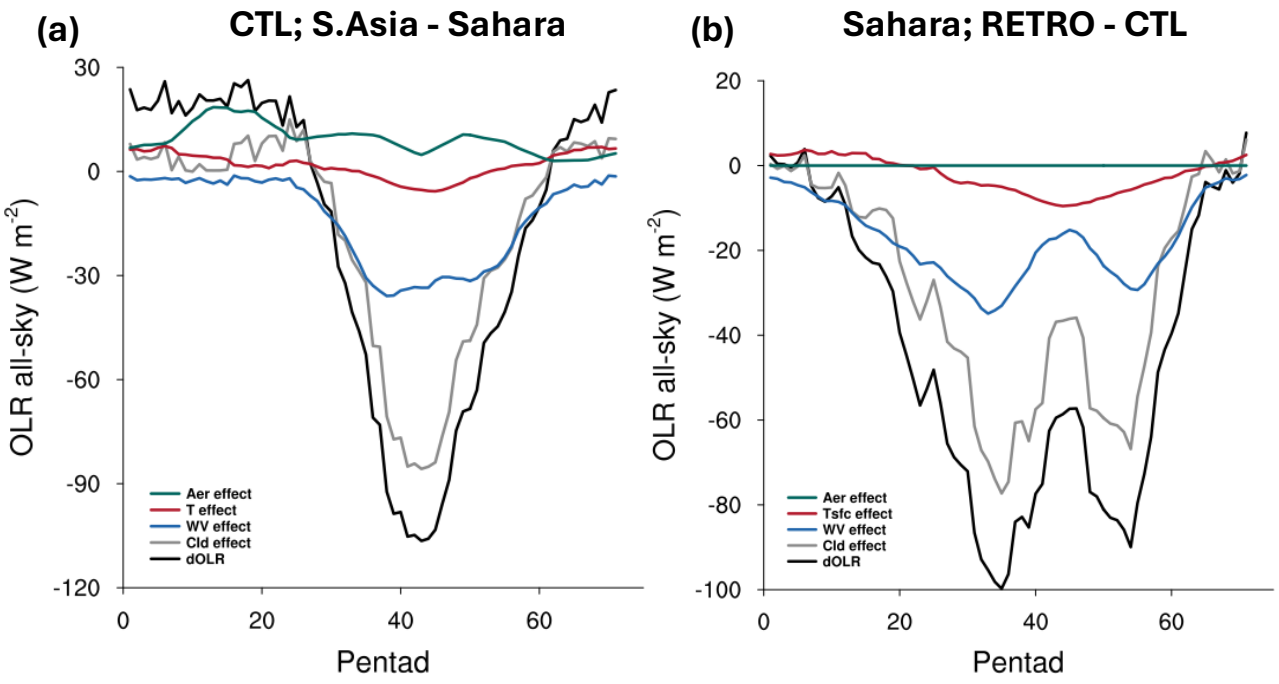

Figure S10. Impact of various factors on OLR. The time series shows the difference in outgoing longwave radiation (OLR) between (**a**) South Asia & the Sahara, and (**b**) RETRO & CTL. The data is represented as follows: black for the total OLR difference, grey for the cloud-related effects on OLR, blue for the radiative effects of water vapor, red for the influence of temperature (both surface and atmospheric), and green for the aerosols. These OLR values are obtained by running the Climlab version of RRTMG in standalone mode, using thermodynamic profiles from the daily climatology of the last 30-years of the simulation. The regions of South Asia and the Sahara are shown in the inset map in Figure 3 of the main text. The region considered for (**b**) is depicted in the inset map shown in Figure 6 of the main text. Following the convention that energy gained by the atmosphere is positive, clear-sky OLR values have been multiplied by -1 to represent energy lost to space.